

# UNGLAZED PHOTOVOLTAIC THERMAL COLLECTORS IN HEAT PUMP SYSTEMS

E. Bertram<sup>1</sup>, M. Stegmann<sup>1</sup>, J. Scheuren<sup>1</sup>, C. Rosinski<sup>2</sup>, K. Kundmüller<sup>2</sup>

<sup>1</sup> Institut für Solarenergieforschung Hameln/ Emmerthal, Am Ohrberg 1, 31860 Emmerthal, Germany,

<sup>2</sup>GEFGA mbH & Co. KG, Löhrgasse 11, 65549 Limburg, Germany, [info@gefga.de](mailto:info@gefga.de)

Corresponding Author: [e.bertram@isfh.de](mailto:e.bertram@isfh.de)

## Abstract

Unglazed Photovoltaic Thermal (PVT) collectors provide very high efficiency for heat and electricity generation at low temperatures. Therefore they are particularly suitable to support the heat source of heat pump systems, where low temperature heat is required. In this combination the PVT collector improves efficiency in two ways- of the heat pump by additional low temperature heat and of the photovoltaic module by lower cell temperatures. An increase of 4% of the annual and up to 9% for the daily photovoltaic electricity production and a high collector yield of 450 kWh/(m<sup>2</sup> a) was measured at a pilot system between April 2009 and April 2010. As the improvement of the PV and heat pump efficiency depends strongly on the thermal PVT collector performance, efficiency measurements of five different unglazed PVT collectors have been carried out. They showed significant differences, e.g. the conversion factor  $\eta_0$  without electricity production varies from 0.33 to 0.73. Further, a simulation model for unglazed PVT -collectors is presented. It is based on thermal performance parameters of EN 12975 and PV performance data at standard test conditions and it further includes thermal collector capacity and condensation effects.

## Introduction

Unglazed PVT collectors improve the efficiency of a ground coupled heat pump system and a photovoltaic (PV) system by combining both via an unglazed PVT collector [1]. So at the same time, the system cools the PV cells, resulting in a higher PV yield with approximately 0.4% per K [6], and heats up the heat pump source or ground. This solution corresponds to a minimum of complexity for the system and the PVT collector design, even if not achieving the maximum possible energy savings for the heat pump system [2]. Nevertheless, the improvement of the total system performance has to justify the additional effort if compared to a side by side heat pump and PV system. For that purpose, measurements of a pilot system are conducted to determine the improvement compared to such a side by side system. This paper focuses on the improvement of the additional PV yield and the general performance of the system. Furthermore, the performance of several PVT collectors has been measured and a detailed unglazed PVT model has been developed for TRNSYS to evaluate the occurring synergetic benefit by simulation studies at different system designs.

## Measurement of PVT Collectors

The thermal performance parameters of a PVT collector determine the annual thermal collector yield and the cooling of the PV in the PVT system. Thus, thermal performance tests on PVT collectors of

five different manufacturers were conducted at ISFH in 2009. All measured collectors are liquid cooled and unglazed/uncovered (no air gap is between the PV cells and the top cover). The thermal performance of the PVT collectors is measured in open circuit operation and described according to EN 12975-2 [3] eq. (1). The performance parameters are discussed on the basis of eq. (2), assuming a constant air speed of 1 m/s. The results are displayed in Figure 1.

$$\eta = \eta_0 \cdot (1 - b_u \cdot u) - \frac{T_m}{G''} \cdot (b_1 + b_2 \cdot u) \quad (1)$$

$$\eta = \eta_{0,u=1} - \frac{T_m}{G''} \cdot b_{u=1} \quad (2)$$

|                 |   |
|-----------------|---|
| $\eta$          | Collector efficiency  |
| $\eta_0$        | Conversion factor   |
| $u$             | air speed of 1 m/s  |
| $b_u, b_1, b_2$ | Performance loss coefficients according to EN 12975 in s/m, W/(m <sup>2</sup> K), Ws/(m <sup>3</sup> K) |
| $T_m$           | Difference of average fluid temperature and ambient air temperature in K                                |
| $G''$           | Net solar irradiance (reduced by infrared radiation balance) in W/m <sup>2</sup>                        |
| $\eta_{0,u=1}$  | Conversion factor for constant air speed of 1 m/s   |
| $b_{u=1}$       | Loss coefficient for constant air speed of 1 m/s in W/(m <sup>2</sup> K)                                |

The measured thermal performance characteristics of the 5 collectors show a strongly different behaviour. The obvious performance differences indicate a clear impact of the collector type to the system. In the following, this impact on the system is discussed by the evaluation of the loss coefficient and conversion factor for the measured PVT-collectors.

In contrast to flat plate collectors the thermal losses of the unglazed PVT collectors are high. Moreover, the front side of unglazed PVT collectors consists of a conventional silicon cell based PV panel. Correspondingly, the optical properties and front side heat loss coefficients are almost identical to a PV module. The collector rear side is different. Two of the investigated collectors have a rear insulation and therefore the lowest loss coefficients (PVT-D and PVT-A with insulation). The differences on the rear side is not only restricted to insulation, but also to the way of integrating the hydraulic piping system onto the PVT rear side. The measured collector loss coefficient  $b_{wind=1}$  varies between 9 and 19 W/m<sup>2</sup>K (PVT-B and PVT-D).

The conversion factor  $\eta_0$  differs in a surprisingly wide range from 0.33 to 0.73 (PVT-B and PVT-D), too. These differences in  $\eta_0$  allow a significant interconnection to the additional PV yield caused by the cooling effect. The influence of  $\eta_0$  is discussed according to eq. (3) by a two node collector model ([4], [5]).

$$\eta_0 = F' \cdot (\tau\alpha) = \frac{U_{int}}{U_{int} + U_{loss}} \cdot (\tau\alpha) \quad (3)$$

|              |  |
|--------------|--|
| $F'$         | Collector efficiency factor  |
| $\tau\alpha$ | Effective transmission-absorption coefficient                                  |
| $U_{int}$    | Internal heat conductivity between absorber and fluid node in W/m <sup>2</sup> |
| $U_{loss}$   | Loss coefficient related to the absorber temperature in W/m <sup>2</sup>       |

Eq. (3) gives a correlation between  $\eta_0$  and  $u_{\text{int}}$  and is valid for constant loss coefficients  $U_{\text{loss}}$ . As the front side of the PVT collectors are almost identical, the transmission/absorption coefficient is approximately constant for all collectors and the thermal losses of this front side are very similar, too. Furthermore, as most of the heat is lost via the front, the change of the overall thermal loss coefficient  $U_{\text{loss}}$  due to different rear side insulations is small if compared to the absolute value of  $U_{\text{loss}}$ . For a rough estimation it is assumed that  $U_{\text{loss}}$  does not differ significantly between the PVT-collectors.

Under these assumptions of a constant  $\tau\alpha$  and  $U_{\text{loss}}$ , eq. (3) gives a clear correlation between  $\eta_0$  and  $U_{\text{int}}$ . A higher  $U_{\text{int}}$  leads to a higher  $\eta_0$ -value. For an identical fluid inlet temperature this higher  $U_{\text{int}}$  value leads to a lower PVT absorber temperature and correspondingly to a colder PV cell temperature. As a result, the collector absorber or cell with the higher  $U_{\text{int}}$  or  $\eta_0$  is cooler for the same collector fluid temperature.

The presented method to evaluate different collectors is a strong simplification which may lead to a false conclusion in case of small  $\eta_0$  differences. Nevertheless, for unglazed PVT-collectors in heat pump systems  $\eta_0$  gives a good orientation for the additional PV yield due to cooling and allows the comparison of different PVT collectors.

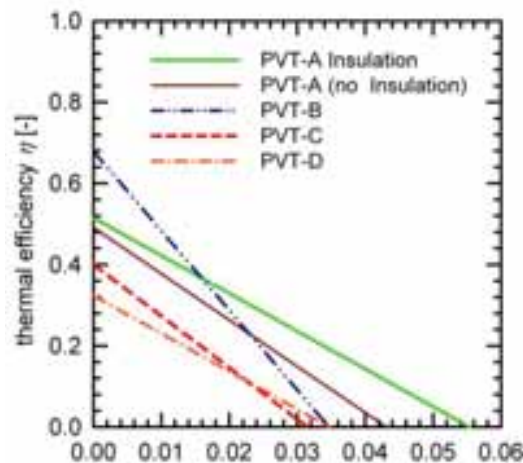


Figure 1: Measured thermal performance for five different unglazed PVT collectors without electricity production. PVT-A was measured with and without insulation on its reverse side.

## Measurement of Heat Pump System

Two benefits result from the application of the PVT collector. The first is the additional PV yield due to the cooling of the PV cells, the second arises for the electrical heat pump performance due to additional heat from the collector.

The impact of an unglazed PVT collector on a heat pump system is investigated in a pilot system. In February 2009, the pilot system was commissioned in near Frankfurt a. M., Germany to supply a large single-family dwelling with heat. The 12 kW heat pump operates together with a PVT collector area of 39 m<sup>2</sup>/5.5 kW<sub>peak</sub> and three tube-in-tube borehole heat exchangers with a total length of 225 m. The PVT collector is connected in series with the borehole heat exchanger by a simple switching valve. In Figure 2 the system concept and a photo of the PVT collector are displayed.

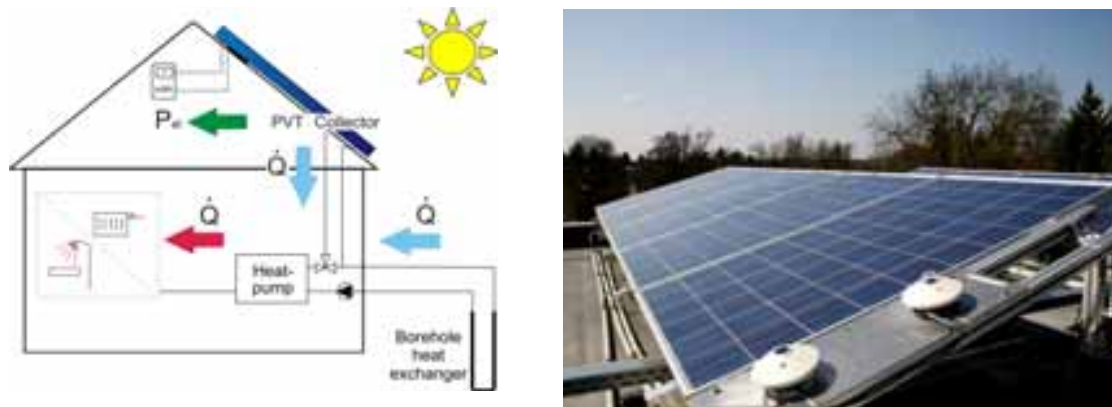


Fig. 2: System concept for the integration of the PVT collector in the heat pump system (left) and a photo of the PVT collector field (right).

The system is analysed for the period from April 2009 to April 2010. During this period the annual thermal collector yield is  $450 \text{ kWh/m}^2$ , of which one third is injected to the borehole heat exchanger and two thirds are supplied directly to the heat pump. Although planned for an annual balance between PV yield and electricity consumption of the heat pump, this is not achieved. The electrical heat pump consumption exceeds by  $1.8 \text{ MWh}$  the total PV electricity production of  $6.7 \text{ MWh}$ . The main reason for the uneven balance in the first place is the extraordinary high heat demand of  $36 \text{ MWh}$  instead of  $27 \text{ MWh}$  according to planning. This high heat demand results from the unexpected high room temperature of about  $23^\circ\text{C}$  in combination with a cold winter. A further consequence is the higher heat extraction from the borehole heat exchanger with  $62 \text{ kWh}$  per m length in comparison to a planned yearly value of  $29 \text{ kWh/m}$ . In summary, this illustrates very clearly the sensitivity of an equal heat and electricity balance to unpredictable impacts like climate, planning faults or behaviour of the user.

The improvement of the PV performance is measured by comparison of the unglazed PVT to conventional PV reference modules operated simultaneously on the same roof. In total, four electrical independent arrays are measured: Two arrays of PVT collectors, consisting of 12 modules each, and two uncooled arrays consisting of two conventional PV modules each. The slope for all PV and PVT modules is  $15^\circ$  with an azimuth angle of  $-24^\circ$  (facing towards south south east).

### Measurement of PVT collector in Heat Pump System

The performance improvement due to cooling effects of the PVT is measured at the system for the period from April 2009 to April 2010. This additional PV yield is measured by comparison of the electrical PVT collector yield against the electrical yield of conventional PV modules. The two PVT collector fields are identical except their rear side insulation. PVT-1 is designed without and PVT-2 with rear side insulation. Both are compared to the two reference PV fields. Between the PVT collectors with and without rear side insulation no significant differences occur. The total yield of the conventional reference modules is  $1043 \text{ kWh/kWp}$ , measured on the primary DC side before the power inverter. Since disturbances occurred, all analysis is carried out for a restricted data range. As disturbances snow, shadows, periods of construction working on-site, and the inaccuracy of the MPP-

tracker below 10% of the nominal power are considered. Due to these restrictions the analysed data cover about 50% of the annual PV yield.

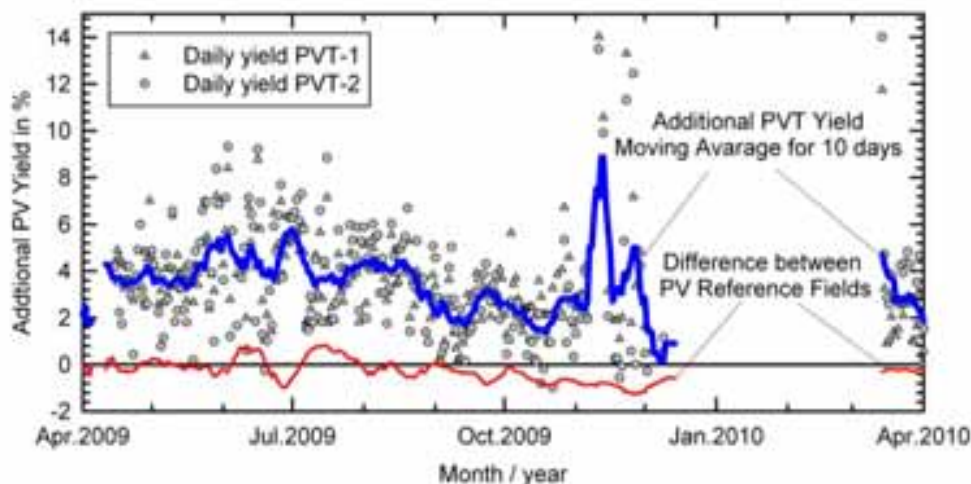


Fig. 3: Measured PV yield for cooled PVT and conventional PV in the course of the year. Displayed are daily and ten day average values

The additional PV yield in the course of the year is displayed in figure 3, where both PVT fields are related to the arithmetic mean value of the PV reference fields. The second line (red) shows the deviation of the measurement for the two identical PV reference fields. The additional yield is discussed in two periods in spring/summer and in autumn. Between the middle of December to the middle of March values are not considered due to disturbances by snow.

In spring and summer the additional daily yields reach values of 9%, although they are significantly varying from day to day. Typical average values are 5 to 6%. In the beginning of autumn the additional yield is lower than in summer. Here 2 to 3% are typical. In the end of autumn very high values of up to 14% in November have been found.

The additional yield in the system depends on the temperature difference between the not cooled and the cooled PV cells. Therefore, high additional yields in summer are obtained only on days with high irradiance and ambient temperature, which leads to hot PV modules in case of no cooling. Further, with rising temperature of the borehole heat exchanger during the summer a slow decrease in August and September compared to June and July may be stated (Figure 3). In the beginning of autumn, two disadvantages coincide. These are a comparatively high borehole temperatures (15°C in September) and low standard PV module temperatures due to lower ambient temperatures and irradiance values. In this period, the lowest cooling benefit within the complete year is achieved.

In the end of autumn, the average heat pump temperature drops to 2°C and at the same time on some days moderate ambient air temperatures occur. Thus, extraordinary high additional PV yields are obtained. As the absolute irradiation in November is negligible, this extra PV yield does not influence the annual result. For the complete year an additional PV yield of 4% has been measured.

In addition to the analysis of a complete year, further information is derived from the evaluation of a single day. In Figure 4, the temperatures for standard PV and the PVT modules are plotted together

with the average fluid temperature for a cloudless summer day. The temperatures are measured on the rear side and on the front glass of the collector or PV segment. Both methods revealed no significant difference. The fluid temperature is the arithmetic average of the collector inlet and outlet temperature.

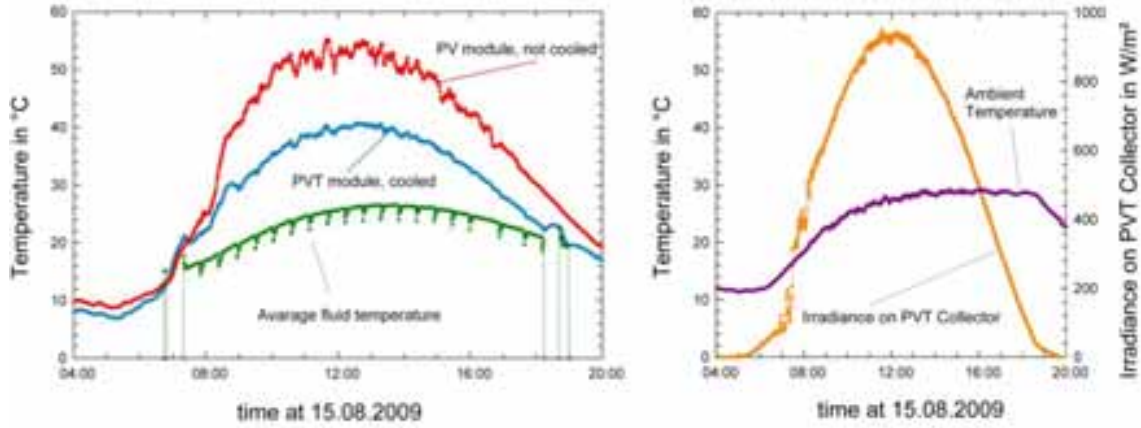


Figure 4: Measurement of the pilot system for a cloudless day: temperatures for PV and PVT collector (left) and ambient temperature and irradiance (right)

As Figure 4 illustrates, the PVT collector reduces the PV temperature clearly by a temperature difference of up to 15 K during noon. Nevertheless the cooling effect in the morning and evening is significantly smaller and typically 5 to 10 K. The energy weighted average temperature  $T_{en-mean}$  is calculated according to eq. (4) to evaluate the temperature influence for the complete day.

$$T_{en-mean} = \frac{\int P_{el,i} \cdot T_i dt}{\int P_{el,i} dt} \quad (4)$$

$T_{en-mean}$  Energy weighted temperature in °C  
 $P_{el,i}$  Measured power in time step i in W  
 $T_i$  Measured temperature in time step i in °C

For the 15<sup>th</sup> of August the energy weighted temperatures are for the standard PV modules  $T_{en-mean,PV} = 46^\circ\text{C}$  and for the PVT modules  $T_{en-mean,PVT} = 34^\circ\text{C}$ . These characteristic temperatures allow the calculation of the relative PV yield improvement  $w_{PVT-PV}$  under the assumption according to Eq. (5) that the improvement of PV efficiency is equal to the improvement of the PV yield  $w_{PVT-PV}$ . Furthermore, the linear expression for the PV efficiency according to eq (6) [6] is used.

$$w_{PVT-PV} = \frac{\eta_{PVT} - \eta_{PV}}{\eta_{PV}} = \frac{W_{PVT} - W_{PV}}{W_{PV}} \quad (5)$$

$$\eta_T = \eta_{STC}(1 - \beta_{STC}(T_T - T_{STC})) \quad (6)$$

$\eta_{PV/PVT}$  Electric efficiency for PV of PVT  
 $W_{PV/PVT}$  Electric yield for PV of PVT in kWh  
 $\eta_{STC/T}$  Electric efficiency at temperature T or 25°C (Standard Test Conditions, STC)  
 $T_{T/STC}$  Temperature at temperature T or at STC in °C

|               |   |
|---------------|---|
| $\beta_{STC}$ | Temperature coefficient related to STC in 1/K   |
| $w_{PVT-PV}$  | Improvement of the PV yield due to cooling in % |

Attention must be paid to the fact that all temperature dependencies are related to STC conditions measured at 25°C. Therefore, eq. (6) has to be combined with eq. (5), resulting in eq. (7), from which the improvement due to cooling can be calculated on the basis of STC values.

$$w_{PVT-PV} = \frac{\beta_{STC} \cdot (T_{PV} - T_{PVT})}{1 - \beta_{STC} \cdot (T_{PV} - T_{STC})} \quad (7)$$

The improvement  $w_{PVT-PV}$  related to the measured uncooled PV yield is then calculated by Eq. (7) with a temperature coefficient  $\beta_{STC}$  of 0.0037 1/K for the PVT modules investigated. The value of 0.0037 1/K is stated by manufacturer and confirmed by ISFH test lab measurement. For the 15<sup>th</sup> of August the additional PV yield due to cooling is determined to 4.8% by the presented temperature method in good accordance to the direct measurement with 4.2%.

In addition to this simple check of the directly measured extra yield, the temperature method allows a calculation of the maximum additional yield for an ideal collector on this particular day. This ideal PVT collector has no thermal resistance between fluid and absorber temperature. Using the same temperature conditions in the system, the coolest temperature which may be achieved is the fluid temperature. On the 15<sup>th</sup> of August the energy weighted fluid temperature is 24°C, which leads to a temperature difference of 22 K. Hence, the maximum possible improvement due to cooling on this particular day is approximately 8.8%, using the simplification, that the mean fluid temperature is not affected by the improved thermal conductance between module and fluid (i.e. improved thermal efficiency). Thus, the realized additional yield on this sunny day may be doubled, if an ideal PVT collector would be installed. In summary, this simple calculation points out three important facts:

1. The presented temperature method gives a good estimation for the additional PV yield due to cooling.
2. Improved collectors with a higher thermal conductance between absorber and Fluid will increase the additional yield up to a maximum, which is defined by the system fluid temperature.
3. Solely a lower fluid temperature may lead to a further improvement.

In contrast to the cloudless day in Figure 4 the PV module temperatures show moderate values if averaged over a longer period. In the year under observation the energy weighted temperature for the standard PV is 33°C, with a measured additional yield of 4%. If the cooling had been reduced the average collector temperature to 12°C, which is the undisturbed soil temperature of the borehole heat exchangers, a maximum temperature difference of 21 K or 8% would be achieved. This indicates that improved PVT designs in combination with an optimised mass flow rate would lead to higher cooling benefits, which however are restricted to maximum twice the measured amount. Furthermore, a special focus on control strategies will lead to lower system temperatures. These aspects are to be analyzed further in dynamic system simulations.

### Unglazed PVT Model

For the mathematical description of the unglazed PVT collector a new TRNSYS model (type) was developed, that is based only on the separately measurable thermal and electrical performance

parameters. The model therefore differs significantly from former PVT collector models. Within the new model the thermal performance is described according to EN 12975-2 for unglazed thermal collectors, while the electrical performance is calculated according to the effective performance model [7] with performance data measured at standard test conditions (1000 W/m<sup>2</sup> at AM 1.5 and 25°C).

The thermal and the electrical model are combined by subtraction of the electrical power from the solar net irradiance  $G''$ . This reduced solar net irradiance  $G''_{red}$  is the input for the thermal model. Additional calculations between the electrical and thermal model are necessary to determine the real PV cell temperature  $T_{cell}$ . These calculations are conducted with the internal thermal conductance  $U_{int}$ , which describes the conductance between fluid and absorber according to eq. (3), and the collector heat flow according to the thermal performance. For most collectors  $U_{int}$  is unknown. Thus, the developed TRNSYS type offers a calculation method from the known thermal collector parameters. Moreover, condensation gains and thermal capacity of the collector are considered by the type. The developed type offers the opportunity to investigate complex questions within dynamic system simulations.

### Acknowledgement

The work presented in this paper has partially been realized within the project “Solare Gebäude-Wärmeversorgung mit unverglasten photovoltaisch-thermischen Kollektoren, Erdsonden und Wärmepumpen für 100% Deckungsanteil – Kurzbezeichnung BiSolar-WP“, (“Solar heat supply for buildings with unglazed photovoltaic-thermal collectors, borehole heat exchangers and heat pumps for 100% solar fraction”), which is funded by the German Ministry for Environment, Nature Conservation and Nuclear Safety (FKZ 0325952). The project is carried out in cooperation with the engineering company GEFGA, Limburg, Germany. The authors are grateful for this support. The content of this publication is in the responsibility of the authors.

### References

- [1] M. Bakker, H.A. Zondag, M.J. Elswijk, K.J. Strootman, M.J.M. Jong., Performance and costs of a roof-sized PV/thermal array combined with a ground coupled heat pump, *Solar Energy*, 78 (2005) 331-339.
- [2] E. Kjellsson, G. Hellström, B. Perers, Optimization of systems with the combination of ground-source heat pump and solar collectors in dwellings, *Energy* (2009), doi:10.1016/j.energy.2009.04.011.
- [3] DIN EN 12975-2, Thermal solar system and components- Solar collectors- Part 2: Test Methods
- [4] J. Duffie, W. Beckman, *Solar Engineering of Thermal Process*, 3<sup>rd</sup> Edition, John Wiley & Sons, Inc. (2006), ISBN-13 978-0-471-69867-8
- [5] Rockendorf G., Bartelsen B., Witt A.: Methods to determine the internal heat transfer coefficient between absorber and fluid of solar collectors. ISES Solar World Congress (1995), Harare
- [6] E.Skoplaki, J.A. Palyvos, On the temperature dependence of photovoltaic module electrical performance: A review of efficiency power correlations.
- [7] A.Wagner, *Photovoltaic Engineering, Handbuch für Planung, Entwicklung und Anwendung*, Springer (2006), ISBN-13 978-3-540-30732-7